Aerospace Science and Technology 39 (2014) 352–360

Contents lists available at ScienceDirect

Aerospace Science and Technology

www.elsevier.com/locate/aescte

Target detection approach for UAVs via improved Pigeon-inspired Optimization and Edge Potential Function

Cong Li, Haibin Duan *

State Key Laboratory of Virtual Reality Technology and Systems, School of Automation Science and Electrical Engineering, Beihang University (BUAA), Beijing 100191, PR China

ARTICLE INFO

Article history:
Received 7 June 2014
Received in revised form 3 September 2014
Accepted 18 October 2014
Available online 22 October 2014

Keywords:
Unmanned Aerial Vehicles (UAVs)
Pigeon-inspired Optimization (PIO)
Edge Potential Function (EPF)
Simulated Annealing (SA)
Target detection

ABSTRACT

In this paper, the hybrid model of Edge Potential Function (EPF) and Simulated Annealing Pigeon-inspired Optimization (SAPIO) algorithm is proposed to accomplish the target detection task for Unmanned Aerial Vehicles (UAVs) at low altitude. EPF can be calculated from the edge map of the original image and provide a kind of attractive pattern for the given target, which is conventionally exploited by the optimization algorithms. Pigeon-inspired Optimization (PIO) is a novel bio-inspired computation algorithm, which was inspired from the homing characteristics of pigeons. In this paper, the simulated annealing mechanism is adopted in our SAPIO algorithm for maximizing the value of EPF. A series of comparative experiments with standard Genetic Algorithm (GA), Particle Swarm Optimization (PSO), Artificial Bee Colony Optimization (ABC) and PIO algorithms demonstrate the robustness and effectiveness of our SAPIO algorithm. Meanwhile, the proposed approach can guarantee accurate target matching.

1. Introduction

Compared with manned aircraft, Unmanned Aerial Vehicles (UAVs) are affordable and convenient for high-risk missions. Today, UAV has been exploited to perform special missions carrying some important equipment such as GPS, optic camera and various sensors [21]. While performing specific tasks, the UAV is an efficient tool because of its superior maneuverability and strong viability [14]. Furthermore, due to the rapid development of artificial intelligence technology, the UAV technology plays a vital role in the technology field of the nation and is essential for improving the security of the society [7,8].

As image sensors have become more and more advanced, it has become imperative to design a satisfying target recognition system for UAVs in order to achieve autonomous reconnaissance and detection. The target recognition and detection method for UAVs has been investigated quite intensively in recent years. Ding et al. [5] used the template matching method to recognize and track runway in the image sequences. Deng and Duan [4] proposed a novel biologically inspired model via improved artificial bee colony and visual attention to perform edge detection. Niu et al. [16] exploit target regions in DWT domain to perform the infrared and visible image fusion, which can make UAV realize environment and perform detection tasks efficiently. Meanwhile, shape representation and matching methods such as Hausdorff distance matching [9] and Charmfer matching [2] are key points in all sorts of ways, and have been extensively adopted for target detection and recognition problems [22].

Energy Potential Function (EPF), firstly proposed by Dao et al., is a novel approach for the edge-based detection in digital images [3]. Similar with the potential generated by the electrostatic field, EPF is exploited to model the potential generated by edge structures of the image. However, EPF is a multi-dimensional and complex function, which is hard to optimize.

In recent years, Evolutionary Algorithms (EAs) including Particle Swarm Optimization (PSO) [17], Artificial Bee Colony Optimization (ABC) [11], and Genetic Algorithm (GA) [10] have become very popular in the optimization community and successfully applied to a wide range of problems. Mirghasemi et al. [15] exploited the combination of the PSO and FCM to solve the sea target detection problem. Wang and Duan utilized the improved version of biogeography-based optimization (BBO) for unmanned helicopter formation [20,18]. Tao et al. used ant colony optimization algorithm and fuzzy entropy for object segmentation [19].

Pigeon-inspired Optimization (PIO) algorithm is a novel swarm intelligence optimization algorithm, which was firstly invented by Duan in 2014 [6]. Motivated by the homing characteristics of pigeons, two operators including map and compass operator and

* Corresponding author. Tel.: +86 10 8231 7318.
E-mail address: hbduan@buaa.edu.cn (H. Duan).

http://dx.doi.org/10.1016/j.ast.2014.10.007
1270-9638/

landmark operator have been designed. PIO algorithm has previously proven itself as a worthy competitor to its better known rivals [6]. However, the basic PIO runs into local optima easily because of its fast convergence. In this study, the simulated annealing [12,1] mechanism is exploited for the generation of the new individual to avoid the local optima. Finally, a novel variant of PIO algorithm, named Simulated Annealing pigeon-inspired optimization optimized (SAPIO), is proposed here.

In this study, the hybrid model of EPF and SAPIO is proposed to accomplish the target detection task for UAVs. The EPF is utilized to provide a pattern of attractive field for the given contour, which is exploited by SAPIO algorithm to optimize the matching procedure. In our work, the EPF is maximized when the given sketch translates, reorients and scales itself to obtain the accurate match. Thus, in this way, the best matching can be obtained.

The remainder of this paper is organized as follows. The main concepts of EPF are introduced in Section 2, while Section 3 describes the basic PIO algorithm and our improved version, respectively. In Section 4, a series of comparative experiments are conducted. Our concluding remarks are contained in the final section.

2. Overview of EPF

EPF is a newly-developed shape-matching approach which was proposed by Dao et al. Similar with the electric potential generated by the electrostatic field, EPF is exploited to model the potential generated by edge structures of the image. The electric potential created by a set of point charges Q_i in a homogeneous background, at a distance r from charges, can be shown to be:

$$v(\vec{r}) = \frac{1}{4\pi\varepsilon}\sum_i \frac{Q_i}{|\vec{r}-\vec{r_i}|} \tag{1}$$

where ε is the permittivity of the medium. $\vec{r}$ and $\vec{r_i}$ are the observation point and charge locations, respectively.

In the EPF model, the ith edge of the image at coordinates (x_i, y_i) is equivalent to the charge point $Q_{eq}(x_i, y_i)$. The edge potential produced by a set of edge points $Q_{eq}(x_i, y_i)$ can be presented as follows [3]:

$$EPF(x, y) = \frac{1}{4\pi\varepsilon_{eq}}\sum_i \frac{Q_{eq(x_i,y_i)}}{\sqrt{(x-x_i)^2+(y-y_i)^2}} \tag{2}$$

where ε_{eq} is the permittivity of the image to be matched. Three kinds of EPF models were proposed by Dao et al., and the Windowed EPF (WEPF) [3] is utilized in this study to reduce the computational complexity, and improve the robustness of the method as well. WEPF simply lies in defining a window beyond which the edge points are ignored. Thus, the definition of the WEPF is written as [3]:

$$EPF(x, y) = \frac{Q}{4\pi\varepsilon_{eq}}\sum_{(x_i,y_i)\in w} \frac{1}{\sqrt{(x-x_i)^2+(y-y_i)^2}} \tag{3}$$

where w is the window chosen; ε_{eq} is the constant permittivity of the image windowed; Q is equal to the charge of each edge points. In this way, the edge potential can be easily calculated from the edge map extracted from the original image. Moreover, the Sobel edge extractor is applied in our study.

In order to determine whether the target image contains the object whose shape is similar to the sketch for a given position, rotation and scale factor, the matching function named EPF energy is defined as [3]:

$$f(c_k) = \frac{1}{N^{(c_k)}}\sum_{n^{(c_k)}=1}^{N^{(c_k)}} \left\{EPF\left(x_n^{c_k}, y_n^{c_k}\right)\right\} \tag{4}$$

Eq. (4) defines the average value of the EPF energy, which represents the degree of the sketch attracted by the target image. Additionally, the EPF is maximized when the given sketch translates, reorients and scales itself to obtain the accurate match. However, EPF is a multi-dimensional and complicated function, which is hard to optimize. Therefore, it is significant to select the appropriate optimization algorithm in this study.

3. PIO algorithm and its improved version

PIO algorithm is firstly proposed by Duan and Qiao [6] and derived from the homing behavior of pigeons. As presented in [6], the rudimentary process of the basic PIO can be described as follows:

First, each pigeon X_i with the initial velocity V_i is randomly initialized within the solution space, denoted as $X_i = [x_{i1}, x_{i2}, ..., x_{im}]$, where i is the ith pigeon, and m is the dimension of the problem to be solved. The rate of the position change (velocity) for pigeon i is represented as $V_i = [v_{i1}, v_{i2}, ..., v_{im}]$. In this study, the rotation, translation (along the horizontal, t_x, and vertical, t_y, directions, respectively) and scaling of the given sketch are parameters to be optimized. Subsequently, the transformed sketch is fitted within the potential field to compute the matching index, namely, the fitness value of the pigeon.

In the individual updating process, two operators are designed for simulating the homing characteristics of pigeons, which are the map and compass operator and the landmark operator, respectively. At the initial moment, suppose the best position of all the pigeons is guaranteed by using map and compass operator, thus each pigeon adjusts its course following the best position [6]. In this map and compass operator, the pigeons are manipulated by the following equations:

$$V_i(t) = V_i(t-1)\cdot e^{-Rt} + rand\cdot\left(X_g - X_i(t-1)\right) \tag{5}$$

$$X_i(t) = X_i(t-1) + V_i(t-1) \tag{6}$$

where R is the map and compass factor which can slow the velocity of pigeons down as the iteration goes, *rand* denotes a random number within $[0, 1]$, and X_g signifies the best position of all the pigeons.

In the landmark operator, suppose that pigeons fly for a certain amount of time but are still far from the destination, which rely on the landmark neighboring [6]. Furthermore, it supposes that pigeons would fly straight to the landmarks where they are familiar, and others would follow those that are familiar to the landmarks. Thus, in Duan's model, the center of all pigeons is their destination in the tth iteration, which can be written as [6]:

$$X_c(t) = \frac{\sum_{Np} X_i(t)\cdot fitness(X_i(t))}{\sum fitness(X_i(t))} \tag{7}$$

where N_p is the number of pigeons in the tth iteration, which is halved in the process above. Specifically, half of the pigeons away from the landmark will follow the other half close to the landmark, which also signifies that two pigeons may be at the same position. In this landmark operator, the pigeons are manipulated by the following equations [6]:

$$X_i(t) = X_i(t-1) + rand\cdot\left(X_c(t) - X_i(t-1)\right) \tag{8}$$

PIO algorithm has been proven to be robust and reliable when it is applied to solve air robot path planning problem [6]. However, when we deeply think about the PIO process above, the basic PIO algorithm has some drawbacks that limit its further application.

In the model of the basic PIO, the landmark operator of the original PIO is conducted in the last few generations. However, the algorithm could be already convergent thus the landmark operator

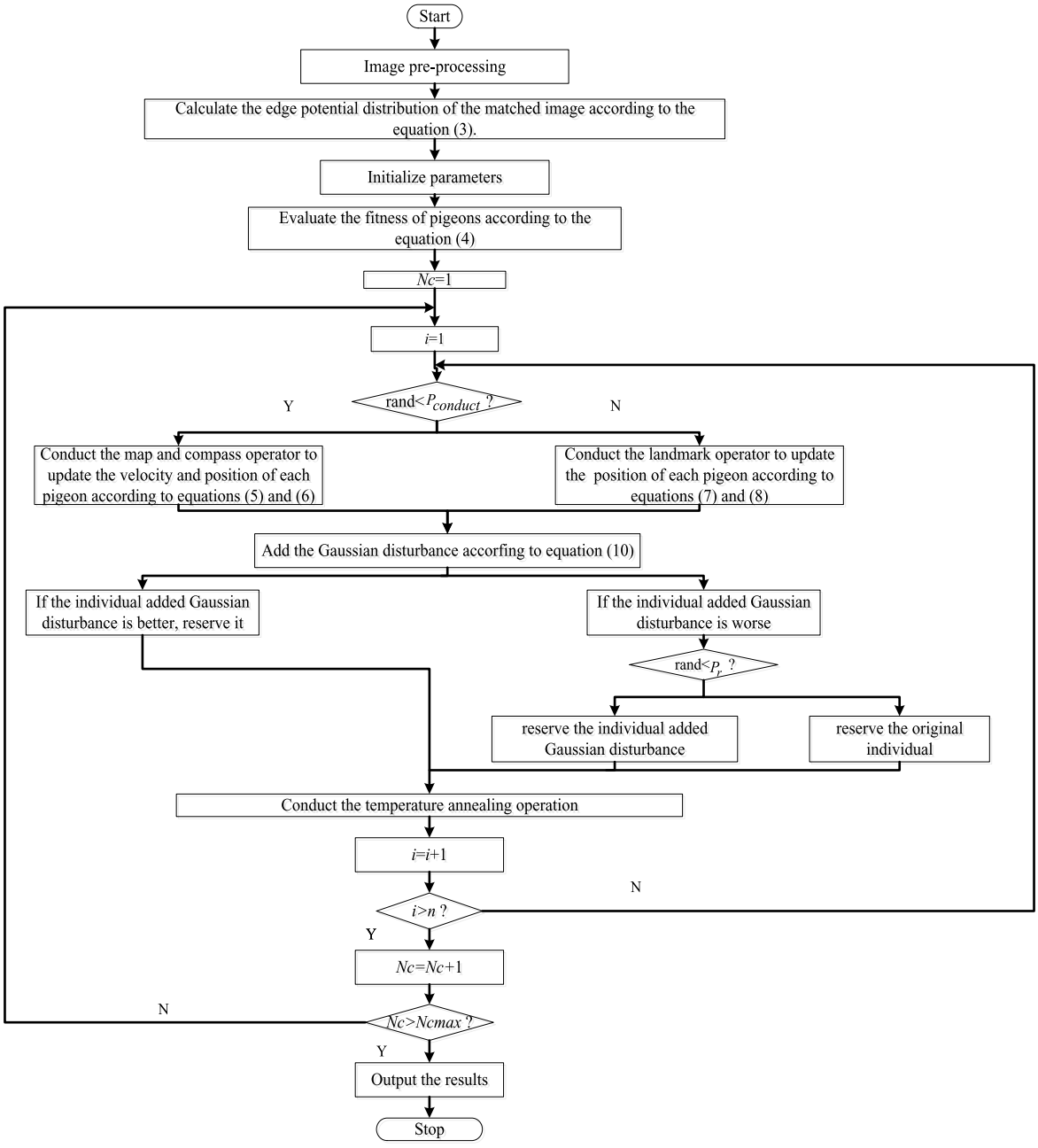

Fig. 1. Detailed flow chart of SAPIO.

Table 1
Set of parameters for SAPIO algorithm.

Parameter	Description	Value
n	Number of pigeons	200
$Nc_{\max}$	Maximum times of iteration	200
R	The map and compass operator	0.2
D	Dimension of the search problem	2
μ	The mean of the Gaussian function	0
σ	The variance of the Gaussian function	1
k	The slope of the log sig() functions	20
T	The initial temperature	1000
C	The temperature decay coefficient	0.5

could not work. In our model, a probability $P_{conduct}$ is exploited, which is defined as:

$$P_{conduct} = \log\mathrm{sig}\left(\frac{Nc_{\max}/2 - t}{k}\right) \tag{9}$$

where log sig() denotes a logarithmic sigmoid transfer function, $Nc_{\max}$ is the maximum iteration number, t is the current iteration number, and k is changing for the slope of log sig() function, which is set as 20 in this study. In each iteration, a random number within $[0, 1]$ is generated to be compared with the $P_{conduct}$. If the random number is less than the $P_{conduct}$, the map and compass operator is conducted. Else, the landmark operator is carried out. Moreover, while conducting the landmark operator, the number of pigeons is reduced by ninety percent in the SAPIO. Since the value of the $P_{conduct}$ decreases from 1 to 0 nonlinearly, there is a higher probability to perform the map and compass operator at the initial moment. Then, the value of the $P_{conduct}$ get smaller as the iteration goes, leading to a higher probability to conduct the landmark operator.

As the search behavior of pigeons only use the best position of all the pigeons, although performed with a fast convergence, it seems easy to get into local optima. In order to avoid the local

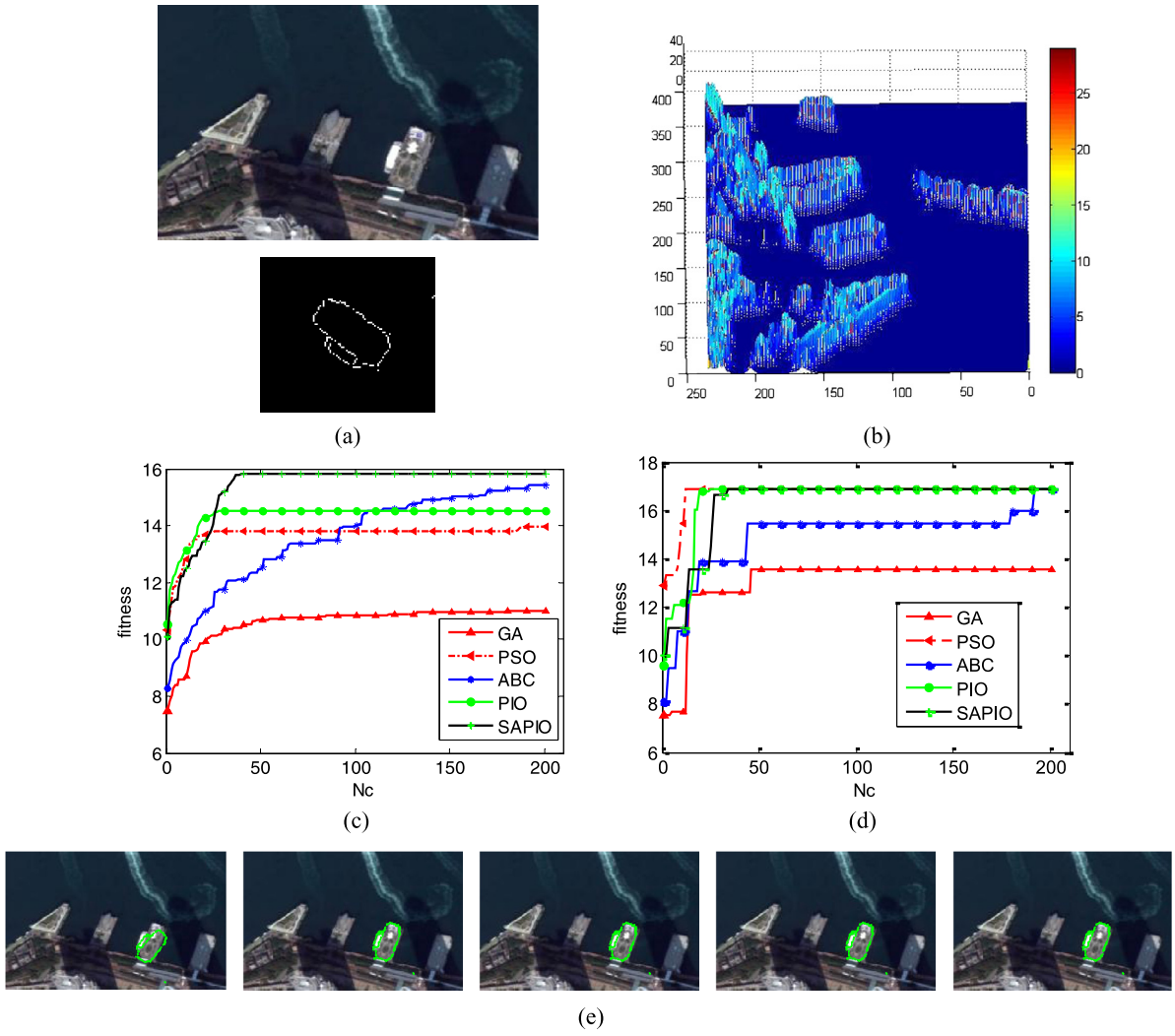

Fig. 2. Experiments of case 1. (a) Original image and the target sketch; (b) The energy potential distribution of the original image; (c) Comparative evolution curves of the mean value of the objective function; (d) Comparative evolution curves of the best value of the objective function; (e) Comparative results of target detection and matching using GA, PSO, ABC, PIO, SAPIO, respectively.

Table 2
The comparative results of GA, PSO, ABC, PIO and SAPIO for case 1 in 10 runs.

Algorithm	Best fitness	Best parameter	Mean
GA	13.5656	(132, 224, 267, 1.2)	10.9862
PSO	16.8679	(119, 225, 286, 1.3)	13.9812
ABC	16.8679	(119, 225, 286, 1.3)	15.4111
PIO	16.8679	(119, 225, 286, 1.3)	14.5277
SAPIO	16.8679	(119, 225, 286, 1.3)	15.8120

Table 3
The comparative results of GA, ABC, PSO PIO and SAPIO for case 2 in 10 runs.

Algorithm	Best fitness	Best parameter	Mean
GA	11.3785	(6, 224, 315, 1.5)	8.9066
PSO	15.8354	(4, 224, 315, 1.3)	8.9721
ABC	15.8354	(4, 224, 315, 1.3)	9.5363
PIO	15.8354	(4, 224, 315, 1.3)	9.2387
SAPIO	15.8354	(4, 224, 315, 1.3)	11.8061

optima with higher efficiency, the Gaussian factor and Simulated Annealing (SA) mechanism are exploited to improve the performance of the basic PIO.

SA was firstly proposed in the 1980s to solve the combination optimization problems [12]. In our model, the Gaussian disturbance is added to the newly-generated pigeons, enhancing its local optimization ability. In addition, as iteration proceeds, the Gaussian factor is supposed to apply a small disturbance with a higher probability. Thus, individuals added Gaussian disturbance can be expressed as:

$$X_{ig}(t) = X_i(t) + \log\mathrm{sig}\left(\frac{Nc_{\max}/2 - t}{k}\right)N(\mu, \sigma) \tag{10}$$

where $\log\mathrm{sig}()$ denotes a logarithmic sigmoid transfer function, which decreases the amplitude of the Gaussian disturbance as the iteration proceeds.

In the model of the SA, the worse individual is reserved with the probability P_r. In this study, suppose that the difference between the fitness of the individual added Gaussian disturbance X_{ig} and the old one X_i is Δf, and the EPF based matching is the maxim optimization problem, then the probability P_r is defined as [12]:

$$P_r = \exp(\Delta f / T) \tag{11}$$

where T is the annealing temperature, which decreases as the iteration goes. In case that the initial temperature is high enough and the annealing rate is low, the improved algorithm contributes to the jumping out of the local optima.

The implementation procedure of our SAPIO optimized EPF can be described as follows:

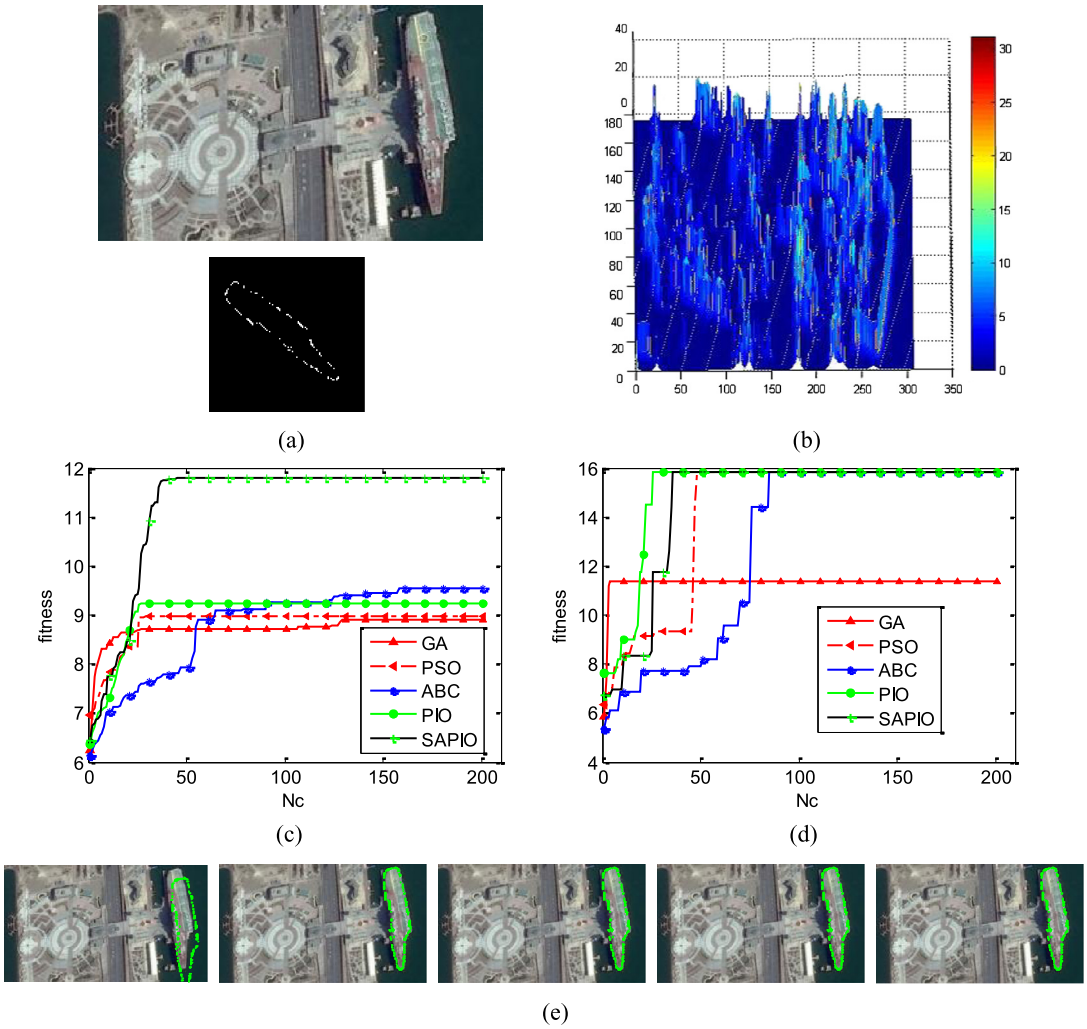

Fig. 3. Experiments of case 2. (a) Original image and the target sketch; (b) The energy potential distribution of the original image; (c) Comparative evolution curves of the mean value of the objective function; (d) Comparative evolution curves of the best value of the objective function; (e) Comparative results of target detection and matching using GA, PSO, ABC, PIO, SAPIO, respectively.

Step 1: Image pre-processing. Filter the noise of the matched image, and then extract the edge map using the Sobel operator.

Step 2: Calculate the edge potential distribution of the matched image according to Eq. (3).

Step 3: Initialize parameters. Initialize parameters of SAPIO algorithm, such as the number of pigeons n, the solution dimension space D, the maxim number of iteration $Nc_{\max}$ and the initial annealing temperature and so on.

Step 4: Evaluate the fitness of pigeons. The rotation, translation and scaling of the given sketch are initialized in the step 3. Subsequently, the transformed sketch is fitted within the potential field according to Eq. (4) to compute the matching index, namely, the fitness value of the pigeon.

Step 5: Select the operator to be conducted. Compare with the given probability $P_{conduct}$, if a random value between 0 and 1 is smaller, then perform the map and compass operator. Otherwise, conduct the landmark operator.

Step 6: Update the pigeons. If the map and compass operator is selected, the velocity and position of each pigeon is updated by Eqs. (5) and (6), respectively. Else, utilize Eqs. (7) and (8) to update the individual.

Step 7: Add Gaussian disturbance. Add the Gaussian disturbance to the newly-generated individuals according to Eq. (10).

Step 8: Compare the fitness of pigeons before and after Gaussian disturbance.

a) If the individual added Gaussian disturbance is better, reserve the better individual.

b) If the individual added Gaussian disturbance is worse, and then calculate the difference of them, and determine the probability P_r according to Eq. (11). Subsequently, a random value between 0 and 1 is generated to be compared with P_r. If $rand < P_r$, reserve the worse individual.

Step 9: Conduct the temperature annealing operation.

Step 10: If n pigeons have been generated, go to step 11. Otherwise, go to step 5.

Step 11: Terminate whether the current number of iterations Nc reaches the $Nc_{\max}$. Otherwise, go to step 5.

The flow chart of the SAPIO optimized EPF is shown in Fig. 1.

4. Experimental results and analysis

In order to investigate the feasibility and effectiveness of the hybrid model in this work, a series of experiments are conducted for four different cases. As presented in Ref. [3], Dao et al. compared the GA-EPF model with the optimized HD and CM techniques, and WEPF is the only method to achieve a correct matching in some cases. In addition, SAPIO algorithm proposed in this paper was further compared with other algorithms, i.e., the basic GA, PSO, ABC and PIO. In this study, the control parameters of PIO and SAPIO are shown in Table 1, and the parameters for GA and ABC

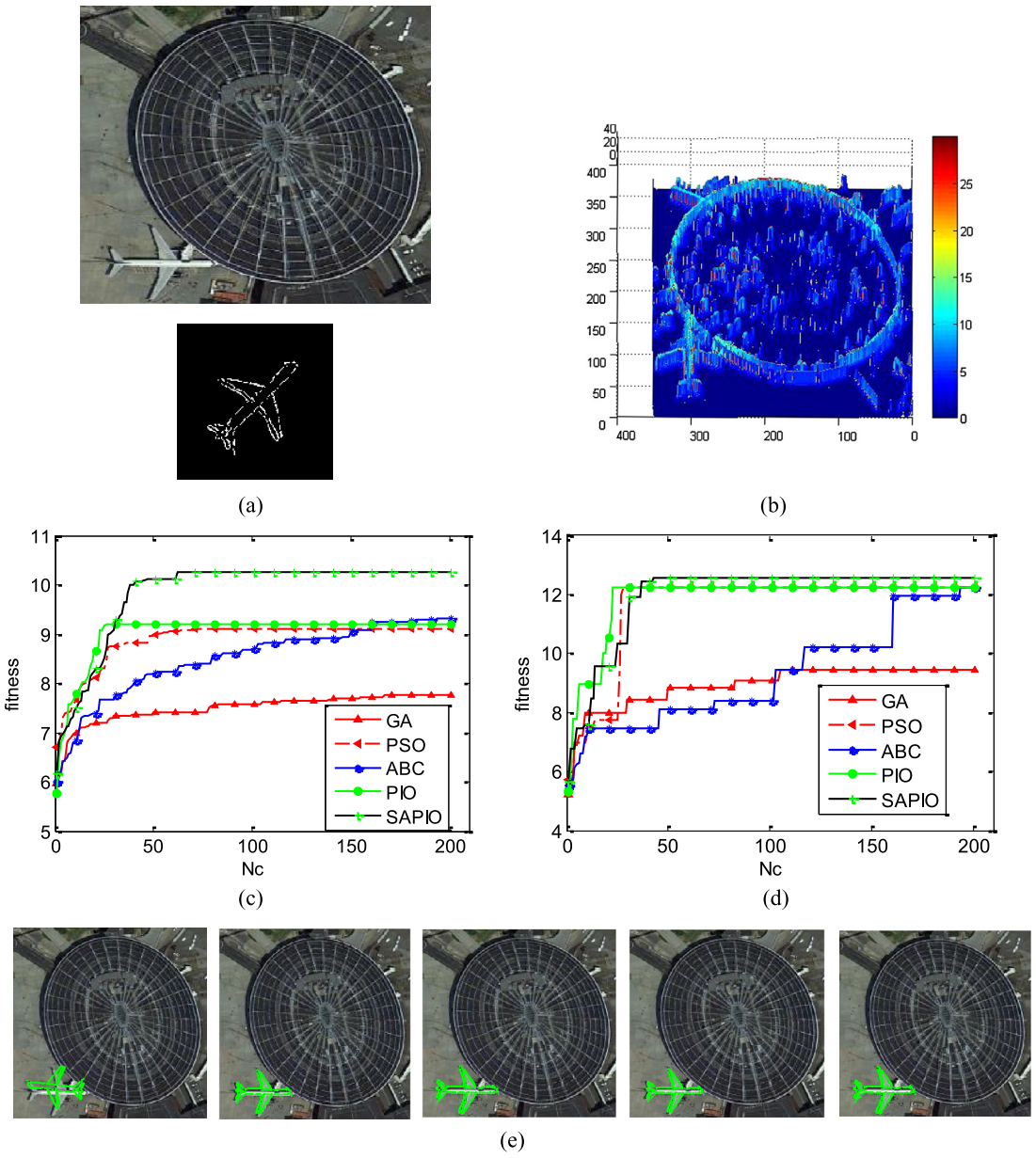

Fig. 4. Experiments of case 3. (a) Original image and the target sketch; (b) The energy potential distribution of the original image; (c) Comparative evolution curves of the mean value of the objective function; (d) Comparative evolution curves of the best value of the objective function; (e) Comparative results of target detection and matching using GA, PSO, ABC, PIO, SAPIO, respectively.

are the same as those in [22]. For SAPIO, the initial temperature is set as 1000 by experimentally. All the pictures used in this paper originate from the Google earth.

The task of the first case is to find the wharf with the specified shape in the original image (Fig. 2(a)). The comparative results of GA, PSO, ABC, PIO and SAPIO for case 1 in 10 runs are presented in Table 2. Additionally, all the following experiments were implemented on a PC with 8 GB RAM using Windows 7 and were encoded in MATLAB 2013b for 64-bit.

From Table 2, it is natural to conclude that the SAPIO outperforms GA, PSO, ABC and PIO obviously, which has the highest mean value in 10 runs among all the algorithms. It should be further noted that GA runs into local optima easily and is not suitable for this case. Moreover, the best matching parameters for SAPIO, PIO, PSO and ABC are the same.

To further compare the SAPIO with other algorithms, the evolution curves of the function's mean value in independently 10 runs for GA, PSO, ABC, PIO and SAPIO are shown in Fig. 2(c) and the best curves of those are compared in Fig. 2(d), respectively. As clearly indicated in Fig. 2(c), PIO has a faster convergence speed compared with the SAPIO algorithm. However, due to the simulated annealing mechanism, it is obvious that SAPIO is more stable compared with the basic PIO from the curve. Moreover, the SAPIO algorithm also converges quickly compared with the ABC algorithm, which indicates it can search the better solution with higher efficiency. Furthermore, it should be noted that GA has the poor performance on case 1. Finally, the satisfactory detection and matching result can be obtained using our method as shown in Fig. 2(e).

Additionally, other experiments are conducted in this study to demonstrate the robustness and effectiveness of our proposed method. Fig. 3, Fig. 4, and Fig. 5 are target detection results of case 2, case 3 and case 4, respectively (see Tables 3, 4 and 5). EPF is multi-dimensional function, and it will generate a vast of local optima when running on clutter background. In that case, matching processes can be stuck forever at one local optima with

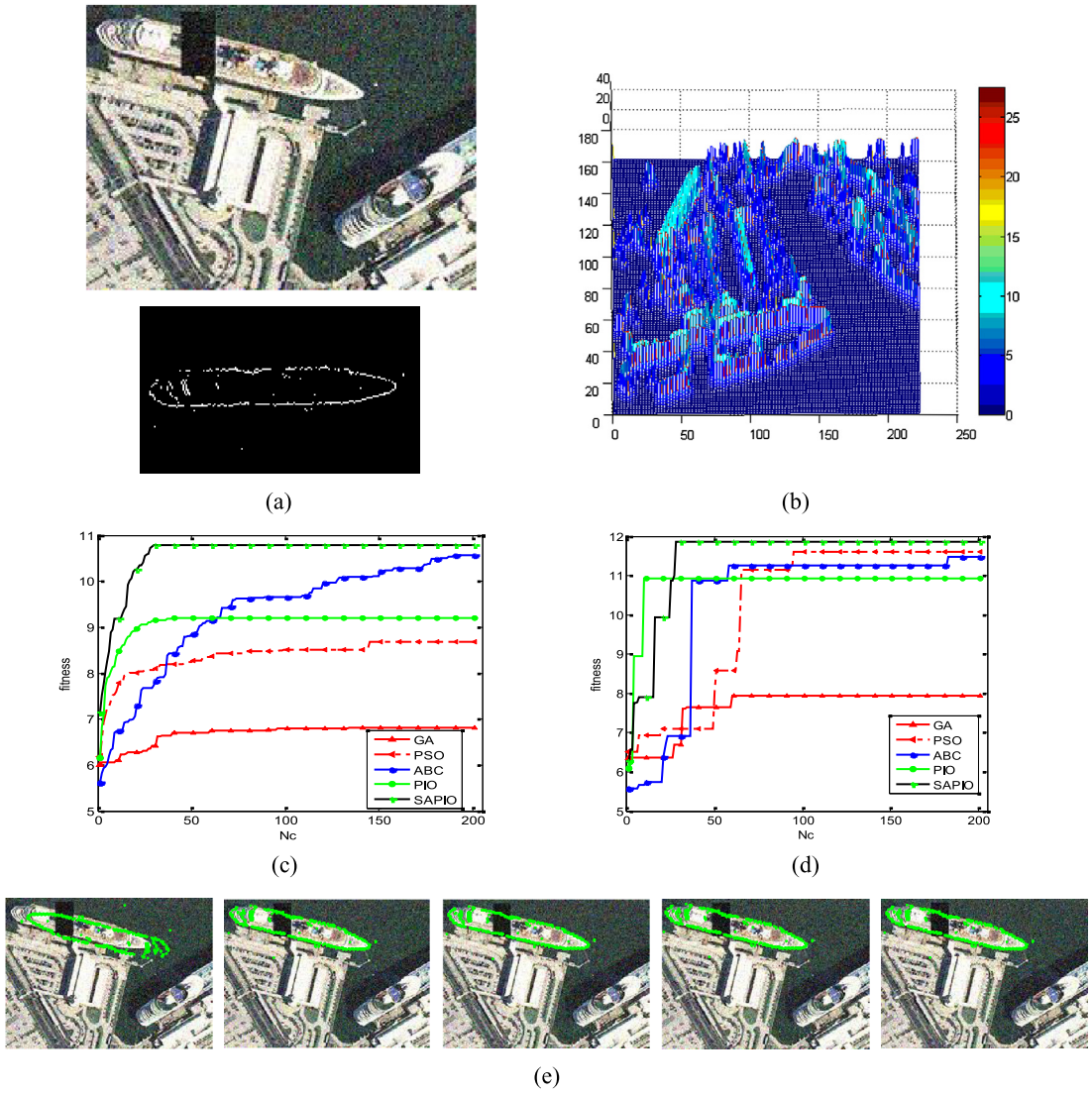

Fig. 5. Experiments of case 4. (a) Original image and the target sketch; (b) The energy potential distribution of the original image; (c) Comparative evolution curves of the mean value of the objective function; (d) Comparative evolution curves of the best value of the objective function; (e) Comparative results of target detection and matching using GA, PSO, ABC, PIO, SAPIO, respectively.

Table 4
The comparative results of GA, PSO, ABC, PIO and SAPIO for case 3 in 10 runs.

Algorithm	Best fitness	Best parameter	Mean
GA	8.1583	(256, 25, 129, 1)	7.7757
PSO	12.2295	(261, 30, 315, 1)	9.0947
ABC	11.9697	(275, 24, 315, 1.1)	9.0907
PIO	12.2295	(261, 30, 315, 1)	9.2084
SAPIO	12.5605	(258, 25, 315, 1.1)	9.9201

Table 5
The comparative results of GA, PSO, ABC, PIO and SAPIO for case 4 in 10 runs.

Algorithm	Best fitness	Best parameter	Mean
GA	7.9405	(7, 17, 165, 1)	6.8155
PSO	11.6076	(6, 4, 345, 1)	8.6832
ABC	11.4713	(7, 3, 346, 1)	10.5777
PIO	10.9333	(5, 1, 345, 1)	9.2051
SAPIO	11.8576	(6, 3, 345, 1)	10.7820

high energy. In order to evaluate the performance of the EPF-SAPIO in clutter background, the original image in case 4 is added with Gaussian noise and the target is occluded partly. From Figs. 3, 4 and 5, it is clear that SAPIO can find the better solution with higher efficiency, though the convergence speed is slower than the original PIO. In addition, the comparative curves show the simulated annealing mechanism can help PIO to escape from possible local entrapment and obtain satisfactory tradeoff between exploration ability and exploitation ability. Moreover, in the case 4, even when the target is in the clutter background and occluded partly, the EPF-SAPIO and EPF-ABC models can detect the target efficiently. However, the convergence speed of the ABC algorithm is much slower than that of the SAPIO algorithm. As a result, the given sketch can translate, reorient and scale itself to obtain the accurate match by using our method even in the clutter background.

Furthermore, we compare our method with the fast directional chamfer matching method [13]. Fast directional chamfer matching approach not only improve the accuracy of matching but also combine the edge orientation information, which was introduced by Liu in 2010 [13]. The detection results of Liu's method for the above four cases are shown in Fig. 6, and the target will be circled with the green square if it could be detected.

It isobvious that Liu's model even cannot detect the target when the given sketch translates, reorients and scales itself. Finally, when the given sketch dose not reorient itself, the results of Liu's model

Fig. 6. Target detection results of the fast directional chamfer matching approach (a) case 1; (b) case 2; (c) case 3; (d) case 4. (For interpretation of the colors in this figure, the reader is referred to the web version of this article.)

Fig. 7. Target detection results when the given sketch does not reorient itself (a) case 1; (b) case 2; (c) case 3; (d) case 4.

Table 6
The comparative computational time for 4 cases (in seconds).

Algorithm	Case 1 Sample (380 ∗ 234) Target (106 ∗ 94)	Case 2 Sample (360 ∗ 175) Target (127 ∗ 127)	Case 3 Sample (360 ∗ 352) Target (147 ∗ 147)	Case 4 Sample (222 ∗ 161) Target (177 ∗ 105)
	Time to run algorithm/iteration			
GA	3.5787	4.9887	6.3198	5.9228
PSO	1.6883	1.9065	2.1558	1.9785
ABC	1.817	2.3415	2.5872	2.5792
PIO	2.0762	2.6531	3.3673	3.0815
SAPIO	2.9347	3.7716	4.1388	3.9765

are presented in Fig. 7. In Fig. 7, only the ship can be detected correctly. Therefore, our proposed method outperforms the fast directional chamfer matching method obviously.

Because UAV always requires real-time processing, and evolutionary algorithms which based on iterations are time consuming, the computational complexity of the proposed method according to the size of image is analyzed in this paper. Table 6 displays the computational time of the proposed methods relevant to the above cases.

From Table 6, it is obvious to conclude that the time to run algorithm is more relevant to the size of the target image, whereas the size of the sample image has a slight effect on the computational time. Although the computational complexity is higher than the original PIO algorithm due to the simulated annealing operation, SA can support PIO to jump out of local optima and the convergence speed of SAPIO is fast. Therefore, it is clear that our proposed SAPIO optimized EPF approach is effective and robust in solving the target detection problem for aircraft at low altitude.

5. Concluding remarks

In this paper, a hybrid biological model of SAPIO algorithm and EPF is proposed to accomplish the target detection and matching task for UAVs. EPF can be calculated from the edge map of the original image and provide a kind of attractive pattern for the given target, which is conventionally exploited by SAPIO. The comparative experiments are conducted among the GA, PSO, ABC, PIO and SAPIO algorithm. Moreover, the simulation results show that the SAPIO clearly improves the performance of the basic PIO owing to the simulated annealing mechanism. Furthermore, the experimental comparison also shows the effectiveness and stability of our method over other algorithms, which provides a more effective way for more complicated UAVs target detection tasks.

Conflict of interest statement

The authors declare no conflict of interest.

Acknowledgements

This work was partially supported by Natural Science Foundation of China (NSFC) under grants #61333004 and #61273054, Graduate Innovation Foundation Award of Beihang University under grants #YCSJ-02-2014-12, Top-Notch Young Talents Program of China, and Aeronautical Foundation of China under grant #20135851042.

References

[1] E. Aarts, J. Korst, Simulated Annealing and Boltzmann Machines: A Stochastic Approach to Combinatorial Optimization and Neural Computing, Wiley, 1989.
[2] G. Borgefors, Hierarchical chamfer matching: a parametric edge matching algorithm, IEEE Trans. Pattern Anal. Mach. Intell. 10 (6) (1988) 849–865.
[3] M.S. Dao, F.G. De Natale, A. Massa, Edge potential functions (EPF) and genetic algorithms (GA) for edge-based matching of visual objects, IEEE Trans. Multimed. 9 (1) (2007) 120–135.
[4] Y.M. Deng, H.B. Duan, Biological edge detection for UCAV via improved artificial bee colony and visual attention, Aircr. Eng. Aerosp. Technol. 86 (2) (2014) 138–146.
[5] M. Ding, Y.F. Cao, L. Guo, A method to recognize and track runway in the image sequences based on template matching, in: Proceedings of the 1st International Symposium on Systems and Control in Aerospace and Astronautics (ISSCAA 2006), 19–21 January 2006, Harbin, IEEE, 2006, pp. 1218–1221.
[6] H.B. Duan, P.X. Qiao, Pigeon-inspired Optimization: a new swarm intelligence optimizer for air robot path planning, Int. J. Intell. Comput. Cybern. 7 (1) (2014) 24–37.
[7] H.B. Duan, S.Q. Liu, J. Wu, Novel intelligent water drops optimization approach to single UCAV smooth trajectory planning, Aerosp. Sci. Technol. 13 (8) (2009) 442–449.
[8] H.B. Duan, S. Shao, B.W. Su, L. Zhang, New development thoughts on the bio-inspired intelligence based control for unmanned combat aerial vehicle, Sci. China, Technol. Sci. 53 (8) (2010) 2025–2031.

[9] D.P. Huttenlocher, G.A. Klanderman, W.J. Rucklidge, Comparing images using the Hausdorff distance, IEEE Trans. Pattern Anal. Mach. Intell. 15 (9) (1993) 850–863.
[10] C.H. Im, H.K. Jung, Y.J. Kim, Hybrid genetic algorithm for electromagnetic topology optimization, IEEE Trans. Magn. 39 (5) (2002) 2163–2169.
[11] D. Karaboga, B. Basturk, A powerful and efficient algorithm for numerical function optimization: artificial bee colony (ABC) algorithm, J. Glob. Optim. 39 (3) (2007) 459–471.
[12] S. Kirkpatrick, Optimization by simulated annealing: quantitative studies, J. Stat. Phys. 34 (5–6) (1984) 975–986.
[13] M.Y. Liu, O. Tuzel, A. Veeraraghavan, R. Chellappa, Fast directional chamfer matching, in: IEEE Conference on Computer Vision and Pattern Recognition (CVPR, 2010), 13–18 June 2010, San Francisco, IEEE, 2010, pp. 1696–1703.
[14] R. Martinez-Val, E. Perez, Aeronautics and astronautics: recent progress and future trends, Proc. Inst. Mech. Eng., C J. Mech. Eng. Sci. 223 (12) (2009) 2767–2820.
[15] S. Mirghasemi, H.S. Yazdi, M. Lotfizad, A target-based color space for sea target detection, Appl. Intell. 36 (4) (2012) 960–978.
[16] Y. Niu, S. Xu, L. Wu, W. Hu, Airborne infrared and visible image fusion for target perception based on target region segmentation and discrete wavelet transform, Math. Probl. Eng. 2012 (2012), 10 pp., http://dx.doi.org/10.1155/2012/275138.
[17] P. Riccardo, J. Kennedy, T. Blackwell, Particle swarm optimization, Swarm Intell. 1 (1) (2007) 33–57.
[18] D. Simon, Biogeography-based optimization, IEEE Trans. Evol. Comput. 12 (6) (2008) 702–713.
[19] W. Tao, H. Jin, L. Liu, Object segmentation using ant colony optimization algorithm and fuzzy entropy, Pattern Recognit. Lett. 28 (7) (2007) 788–796.
[20] X.H. Wang, H.B. Duan, Biologically adaptive robust mean shift algorithm with Cauchy predator–prey BBO and space variant resolution for unmanned helicopter formation, Sci. China Inf. Sci. 2014 (2014) 57, http://dx.doi.org/10.1007/s11432-014-5135-3.
[21] W.R. Williamson, G.J. Glenn, V.T. Dang, S.M. Stecko, J.M. Takacs, Sensor fusion applied to autonomous aerial refueling, J. Guid. Control Dyn. 32 (1) (2009) 262–275.
[22] C.F. Xu, H.B. Duan, Artificial bee colony (ABC) optimized edge potential function (EPF) approach to target recognition for low-altitude aircraft, Pattern Recognit. Lett. 31 (13) (2010) 1759–1772.